Landing Site Selection for the SpaceIL Mission to the Moon

Yuval Grossman, Alexander Novoselsky, Oded Aharonson and the SpaceIL Science Team
Weizmann Institute of Science, Rehovot, Israel

Introduction

Illustration of the SpaceIL lander on the lunar surface (top) and SILMAG - the SpaceIL Magnetometer sensor and electronics (bottom). *With accuracy of 0.1 nT and range of ±8,000 nT, this instrument will measure the lunar crustal magnetic field from orbit, during landing and on the surface.*

Phase 1: Global Filtering

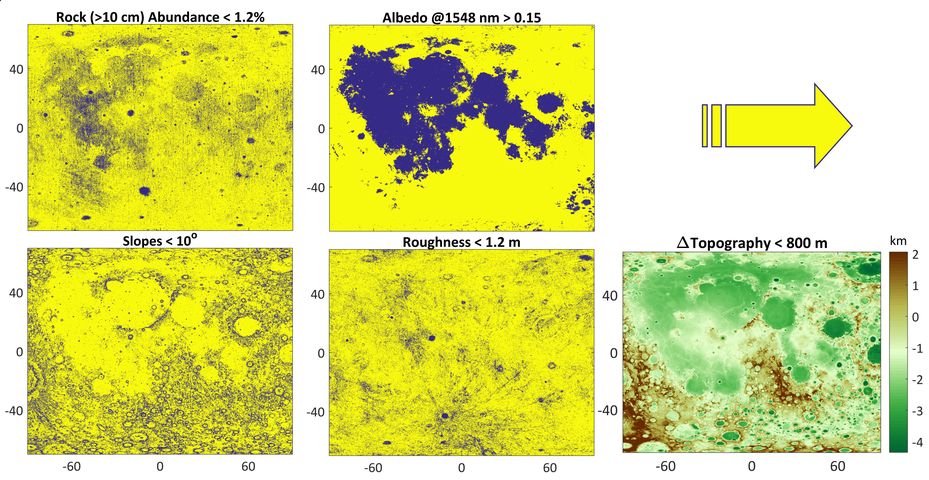

Global Constraints: Global data products we used to verify ground locations (yellow), at a resolution of 16 pix/deg:

Rock Abundance: The LRO Diviner Radiometer provides rock abundance estimates by modeling the surface temperature variations [1,2].

Albedo at wavelength 1548 nm: Spacecraft navigation employs a laser altimeter, imposing a minimum reflectance requirement. We use data acquired by the Selene Multiband Imager Near InfraRed instrument, in the 1548 nm channel.

Surface Slopes and *Roughness*: Slopes from LRO LOLA altimetry data [4,5] and roughness based on root mean square (RMS) of altitude departures from planar fit to consecutive data points [5]. The baseline varies from 30 to 120 meters and the data are binned in areas of 2x2 km.

Maximum topographic variation: The landing system design limits the maximum topographic variations allowed within the landing ellipse. We use the Selene-LOLA derived elevation model SLDEM [3] to impose a criterion of maximum variation from peak to peak.

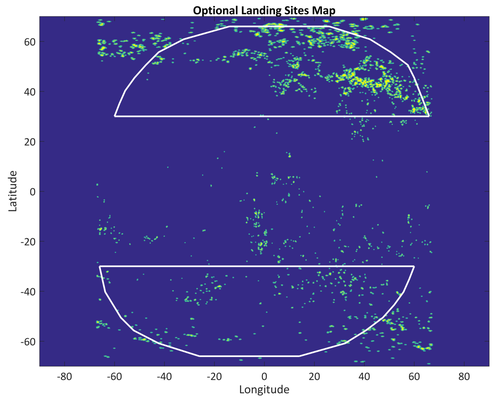

Verified Location Map: If a location meets the above constraints, it is considered as verified. We searched for 15x15 km landing areas were 95% of the area is verified. In addition, we selected sites which have <800 m topography peak-to-peak. The yellow pixels here represents those centers of landing sites, while the green pixels are the surroundings landing ellipses.

Thermal consideration dictate latitude constraints while communication requirements impose longitudinal constraints. The white contour encircle the areas relevant for landing determined by these considerations.

Phase 2: Selecting Candidates Sites

The pool of candidate sites has been sorted by the average magnitude of the magnetic field at the surface and several clusters of sites has been chosen for further detailed analysis.

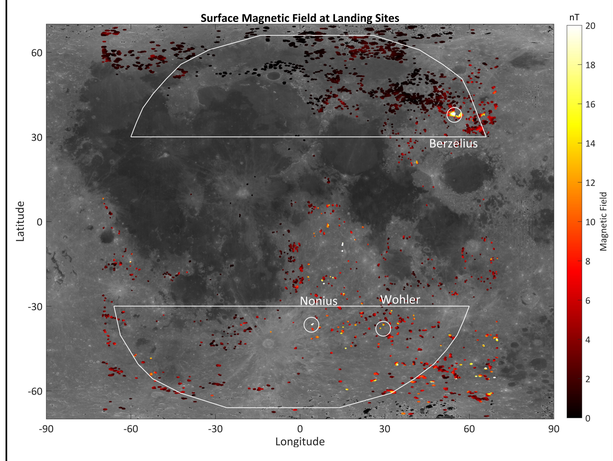

Surface Magnetic Field at Landing Sites: all candidate landing sites on the background of the moon's albedo. Each colored pixel is part of an optional site, while the color represent the magnitude of the magnetic field at the surface. 3 clusters of sites were detailed analysis so far, 2 in the southern hemisphere and 1 in the northern one, as presented below.

Phase 3: Detailed Analysis

Site Berzelius (37.8 N, 53.3 E)

1. Regional Setting

Located in the northern hemisphere in the highlands north of Mare Crisium. Highest magnetic anomaly in the north that fits our constraints.

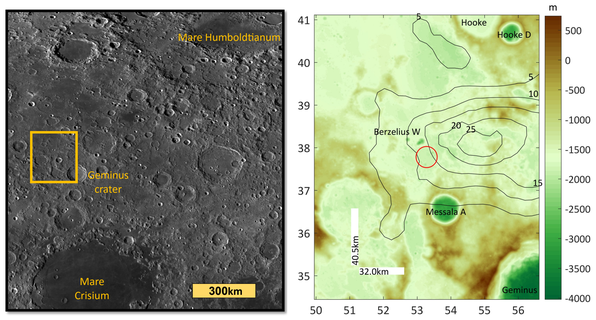

Left - main prominent features in the north-eastern near side of the lunar surface [8]. Right - enlargement of the orange frame - topography map from SLDEM in 128 ppd [3]. The black contours are the magnitude of the surface magnetic field. Red circle is the site analyzed here.

2. Specific Site Selection

This area is a cluster of multiple landing sites. In order to choose preferred candidates within this cluster, the specific location of the centroid of the landing site was chosen such that the peak-to-peak topography is minimized.

The red circle represents the specific site that is analyzed here. The orange rectangles are the footprints of LROC NAC images used for stereo processing and high resolution Data Elevation Model generation.

Additionally, we calculated several numeric measures, based on the data product above, for each site, as specified below.

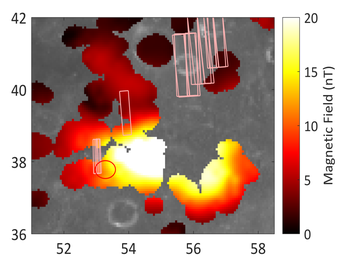

Equivalent Radius	Threshold Pixel Percentage	Mean |B|	STD |B|	Max (99%) ΔTopography	STD Topography
7.55 km	98.4%	11.5 nT	1.91 nT	356 m	48 m

Percentile	Slope (°)	Roughness (m)	RA (%)	Albedo
95	9.12	1.14	0.99	0.18
99.85	12.44	1.58	1.36	0.14

3. Topography, Slopes and Local DTM

The topographic variation in this site is 356 m peak-to-peak, and the standard deviation is relatively low (48 m), due to two relatively deep craters (300 m deep from their surroundings, both with diameter of ~2 km) within the site. The two craters are close to the edge of the landing ellipse and the majority of the site is relatively flat with variation of ~200 m over several km. This is also seen in the slopes map with relatively low RMS value (6.22°).

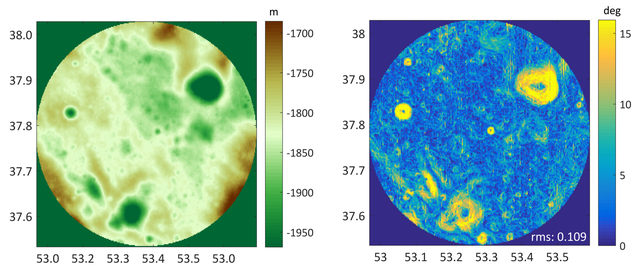

Left - topography from SLDEM in resolution of 512 pix/deg [3]. Right - surface bidirectional slope calculated from the left panel, on scale of ~60 m. Both color bars scaled to 3 sigma range.

This site contain LROC NAC images that fit for stereo processing, thus we generated topographic grid (left) at a resolution of 2 m/pix using SOCET SET [7]. This grid covers the west portion of the site. Note features emerge that were not observable in the global model (the DTM is overlays the global model). We further produce and evaluate a slope map (right) on a baseline of 2 m, most relevant to the spacecraft scale.

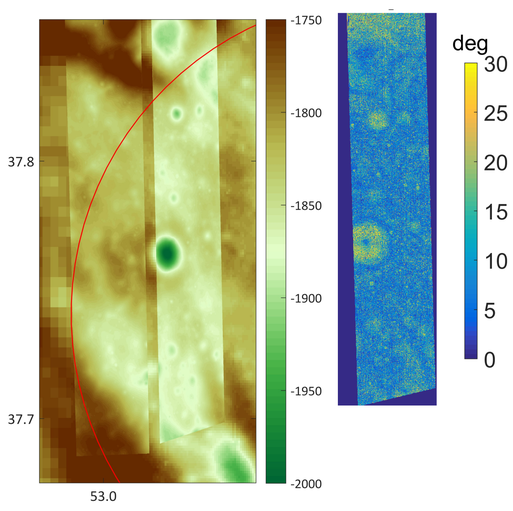

4. Geology

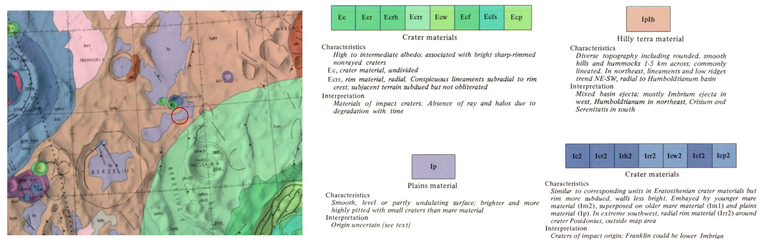

The background geologic unit all over the area, the Hilly-Terra material (Iplh, orange), is made of debris from the Pre-Imbrian giant basins Crisium and Humboldtianum. On top of this unit embedded Plains material (Ip, purple) – smooth, relatively flat surfaces, relatively higher albedo and higher density of small craters (d<3 km) than mare material. Dated to the middle Imbrian period. Origin not clear: might be from volcanic origin, mass-wasting or impact ejecta origin. Near the site lays the ejecta blanket of Geminus crater (Erasthenian period). This unit (Ecrr, green) is rim material, with lineaments subradial to rim crest. Absence of ray and halos due to degradation with time.

5. LROC Narrow Angle Camera High Resolution Images

This site has a full coverage of LROC NAC images in resolutions ranges from 0.4 to 1.5 meters per pixel. In the narrow angle LROC images on the right , craters down to several meters in scale can be seen.

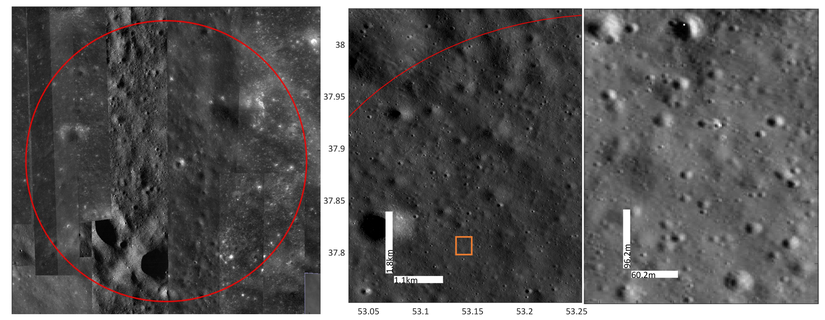

References: [1] Bandfield, J. L. et al. (2011), J. Geophys. Res., 116, E00H02. [2] Shoemaker, E. M. and Morris, E. C. (1970), Radio Sci. 5, 129–155. [3] Barker, M. K. et al. (2016), Icarus, 273, 346-355. [4] Smith et al. (2010), Space Sci. Rev. 150:209. [5] Rosenburg, M. A. et al. (2011), J. Geophys. Res., 116, E02001. [6] Tsunakawa, H., F et al. (2015), J. Geophys. Res., 120, 1160–1185. [7] Tran T. et al. (2010), 41st LPSC, Abstract #2515. [8] LRO WAC Global Mosaic from QuickViewer (http://target.lroc.asu.edu/q3). [9] Geologic map of site Berzelius, taken from the Geologic map of the Geminus Quadrangle of the moon (I-841), M.J. Grolier, 1974. Scale 1:1,000,000.